

Improved axial position detection in optical tweezers measurements

Jakob Kisbye Dreyer, Kirstine Berg-Sørensen, and Lene Oddershede

We investigate the axial position detection of a trapped microsphere in an optical trap by using a quadrant photodiode. By replacing the photodiode with a CCD camera, we obtain detailed information on the light scattered by the microsphere. The correlation of the interference pattern with the axial position displays complex behavior with regions of positive and negative interference. By analyzing the scattered light intensity as a function of the axial position of the trapped sphere, we propose a simple method to increase the sensitivity and control the linear range of axial position detection. © 2004 Optical Society of America

OCIS codes: 040.5160, 040.1880, 120.4640, 140.7010.

1. Introduction

Since the first demonstrations of optical trapping of dielectric particles, optical traps, also known as optical tweezers, have become an important tool in biophysics and colloidal science: see Ref. 1 for a recent overview of the literature. In many cases measurements of the lateral position of the trapped object, i.e., the position in the direction perpendicular to the laser beam, give information sufficient for probing the system of interest. There are, however, applications where knowledge of the position in all three dimensions would contribute significantly to the understanding of the system. For example, three-dimensional position detection might considerably improve measurements of the diffusion constant of proteins in the bacterial outer membrane, such as in Ref. 2. In such experiments the motion of the protein in the membrane is likely to have significant components out of the lateral plane because of the relatively small radius of curvature of the bacterium. In other experiments the forces investigated may have small, but significant, axial components.³ Often, axial position detection relies on extrinsic methods, such as total internal reflection microscopy⁴ or two-photon excitation.⁵

One commonly used method for determining both axial- and lateral position of an object in an optical trap is to measure the intensity of the forward-scattered light with a quadrant photodiode placed in the back focal plane of the microscope condenser. In this case, for small fluctuations of the bead, the lateral x - and y -coordinates of the trapped bead are proportional to the differences in light intensity on the four quadrants,⁶ and within a certain regime the axial position is proportional to the fluctuations in the sum of the intensities on the quadrants.^{7,8} Here we report a new experimental approach to back-focal-plane detection with emphasis on resolving the axial positions of the bead. We show that, through deeper understanding of the back-focal-plane interference pattern, the signal-to-noise ratio and the linear range of detection can be controlled and optimized.

2. Experimental Setup

The optical tweezers setup consists of a Nd:YVO₄ laser operating at a wavelength of 1064 nm (10 W, Spectra Physics Millennia), which is directed into an inverted microscope (Leica DMIRBE). The laser output is expanded with a commercial beam expander (20×, Casix) and passes a half-wave plate and a beam-splitter cube used for attenuation of the laser beam. Two mirrors serve to steer the beam during the alignment. Before entering the microscope, the beam is focused by a lens, L₁ ($f = 35$ cm), that compensates the defocusing of the built-in microscope tube lens, L₂ ($f = 25$ cm).

The essential components, including L₁ and L₂, forming the optical trap and the detection system are depicted in Fig. 1. The trap is formed by the micro-

The authors are with the Niels Bohr Institute, Blegdamsvej 17, DK-2100 Copenhagen, Denmark. J. K. Dreyer's e-mail address is kisbye@nbi.dk.

Received 11 September 2003; accepted 17 December 2003; revised manuscript received 6 January 2004.

0003-6935/04/101991-05\$15.00/0

© 2004 Optical Society of America

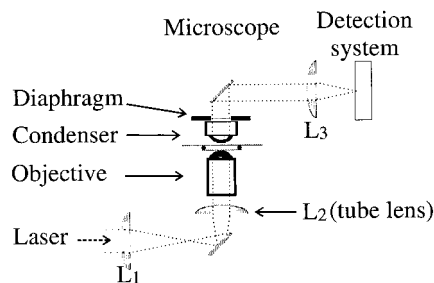


Fig. 1. Schematic illustration of the components forming the optical tweezers and the detection system. The laser beam enters the microscope via the side port, and the built-in tube lens, L_2 , must be incorporated into the optical path. Lens L_3 images the back focal plane of the condenser onto the detection system, either a quadrant photodiode or a CCD camera. In this figure the beam expander, mirrors, and attenuating system have been omitted.

scope objective (100 \times , oil, numerical aperture NA = 1.4). The forward-scattered light from the sample is collected by the microscope condenser (oil, NA = 1.4, diameter 22 mm). The back focal plane of the condenser is imaged by a lens, L_3 ($f = 3.75$ cm, diameter 25.4 mm), onto either a quadrant photodiode (Hamamatsu S5981) or a CCD camera (Sony XC-75CE, frame rate 25 Hz). Lens L_3 is placed 19.9 cm along the optical path from the condenser and 4.2 cm from the detector. The sample is mounted on an xyz piezo translation stage (Physik Instrumente, P-517.3CL); before entering the CCD camera, the laser beam is attenuated by an absorptive neutral-density filter (Thorlabs ND40B). Except where indicated, measurements have been performed on polystyrene microspheres dissolved in deionized water.

3. CCD-Image Analysis

Inserting a CCD camera into the back focal plane of the condenser instead of the quadrant photodiode yields more detailed information on the interference pattern of the forward scattered light. Figure 2(a) shows a CCD image of the back-focal-plane interference pattern of a trapped bead. The image appears as a bright disk, as only light at angles less than the critical angle of the glass-water interface at $\theta_c = 61$ deg is detected from the sample. At each pixel the angle θ is defined as $\sin(\theta) = r/f$, where r is the radial distance from the image center to the pixel. The constant f is given by $f = r_c/\sin(\theta_c)$, where r_c is the radius of the disk of the interference pattern. The presence of a bead in the optical trap is seen as a dark shadow in the image center.

From the CCD camera, a recording of 1500 consecutively sampled frames of a trapped bead undergoing Brownian motion were analyzed to find their information content regarding the axial position of the trapped bead. The axial root-mean-square deviation of the bead from the mean position was ≈ 50 nm, and the mean distance from the coverslip to the bead was approximately 3 μm . We investigate the corre-

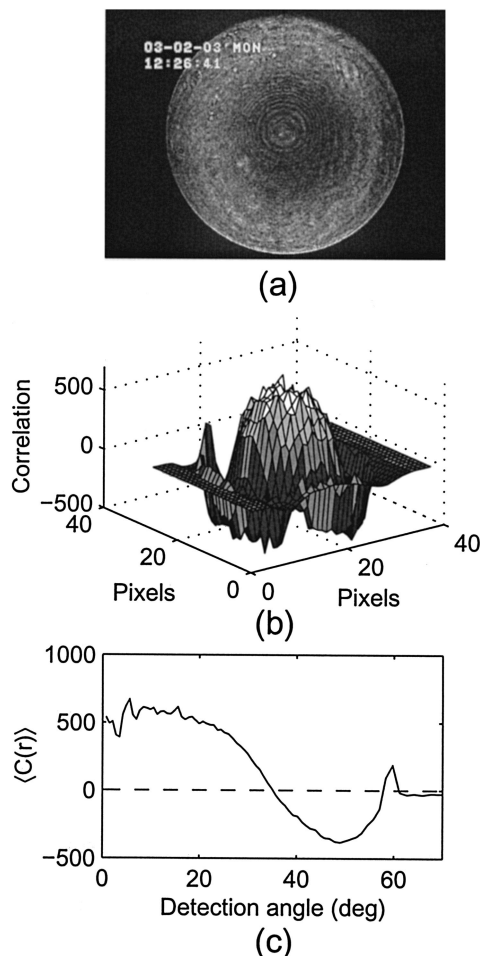


Fig. 2. Analysis of forward-scattered light detected with a CCD camera. (a) Interference pattern of a trapped bead (diameter 1.07 μm). The physical diameter of the image is 5 mm. (b) Corresponding correlation matrix, C of Eq. (1). Each surface element in the plot is the mean of 5×5 entries of C . (c) Mean value of the correlation matrix C as a function of the detection angle θ . At angles θ below 35 deg, the light intensity of the image in (a) increases as the bead moves along the axis of the laser beam. At angles from 35 to 58 deg the correlation is negative, while a peak of positive correlation is visible close to the critical angle at 61 deg.

lation of each pixel intensity with respect to the total intensity,

$$C_{kl} = \langle p_{kl}^i \Sigma_i \rangle - \langle p_{kl}^i \rangle \langle \Sigma_i \rangle. \quad (1)$$

Here, $p_{kl}^i \in \{0, \dots, 255\}$ is the intensity recorded at the pixel with indices k and l in image number i , and Σ_i is the sum of all pixel intensities in image i . The mean value is taken over all images in the recording. By moving the bead in a well-controlled fashion in the axial direction, the total intensity, Σ_i , was found to be proportional to the axial position of the bead, z , as on the quadrant photodiode.^{7,8}

In Fig. 2(b) a surface plot of the correlation matrix C is shown. It shows that the intensity in the middle of the image is positively correlated with the z position of the bead. Further from the center, the sign changes and the intensity becomes negatively

correlated with the z position. Figure 2(c) shows the average of the correlation matrix in a rim $d\theta$ as a function of θ . In this figure the region of positive correlation at low scattering angles and the region of negative correlation at angles above $\theta \approx 35$ deg are clearly distinguishable. In addition, a distinct positive peak develops at the critical angle. At angles greater than 61 deg, the condenser receives no light from the sample, and the correlation drops to 0. Note that in Fig. 2(c) the number of pixels that contribute to the average increases with θ . Figure 2 clearly illustrates that integrating the intensity of the entire accessible area of the photodiode will decrease the amount of information on the axial position, as regions with both negative and positive correlations are included and their contributions to the total intensity cancel. As is shown below, the total contributions from the positively and negatively correlated areas may even exactly cancel, and as a result the total axial signal vanishes. This result holds for beads of size 0.4, 1.07, and 2.3 μm .

4. Photodiode Response

For various capture angles, θ_{cap} , of the condenser, we investigated the response of the quadrant photodiode and determined in which range this signal was proportional to the axial position of the bead. The angle θ_{cap} is the opening angle of the light cone detected by the condenser and can be easily adjusted with the condenser aperture diaphragm placed immediately above the condenser on the microscope; see Fig. 1. We induced oscillations in the position of the bead relative to the optical trap by oscillating the surrounding medium with the piezo stage. The equilibrium position of the bead was set to be approximately 6 μm above the coverslip of the sample, and the laser intensity was kept at the lowest possible that could hold the bead trapped. Under these circumstances the bead is influenced by an external force of magnitude $F_{\text{ext}} = -\gamma v$, where the drag coefficient, γ , is found from Stokes Law, $\gamma = 6\pi\eta r$. Here η denotes the fluid viscosity, r the radius of the bead, and v the velocity of the bead with respect to the medium. Let Z_{bead} and Z_{sample} denote the coordinates of the bead and the sample relative to the trap, with the axis oriented in the same direction as the propagation of the laser beam. The potential exerted by the trap is approximately harmonic with spring constant κ_z .^{4,7,9} The motion of the trapped bead can then be described by

$$\gamma \dot{Z}_{\text{bead}} + \kappa_z Z_{\text{bead}} = \gamma \dot{Z}_{\text{sample}}. \quad (2)$$

In the present case, $Z_{\text{sample}}(t) = A \sin(2\pi f_0 t)$, with $A = 1.29 \mu\text{m}$ and $f_0 = 40 \text{ Hz}$. The response of the trapped bead was sampled at 4 kHz with the photodiode and can be found from Eq. (2) to be $Z_{\text{bead}}(t) = A' \sin(2\pi f_0 t + \phi)$, with amplitude $A' = A[1 + (\kappa_z/2\pi\gamma f_0)^2]^{-1/2}$ and phase $\phi = \tan^{-1}(\kappa_z/2\pi\gamma f_0)$. From power spectral analysis, the ratio $\kappa_z/2\pi\gamma$ was found to be $3.80 \pm 0.15 \text{ Hz}$.¹⁰ Consequently, the ratio of the amplitudes is determined to be $A'/A = 0.996$, and the phase lag $\phi = 5.4 \text{ deg}$. A direct measurement

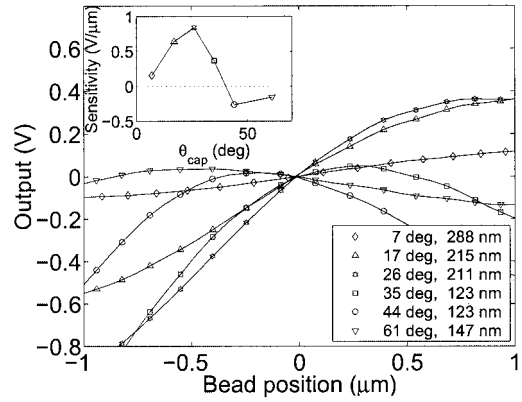


Fig. 3. Total intensity on the quadrant photodiode with respect to the axial position of the trapped bead (diameter 1.07 μm). The legend provides the capture angle of the condenser, θ_{cap} , and the total range of linear detection. The inset shows the sensitivity of the axial position signal defined as the slope of the photodiode signal at the equilibrium position.

gave $\phi = 3.6 \text{ deg}$. The deviation between the two values of ϕ could be caused by the fact that the trapped bead is forced to extreme positions where the assumption of a harmonic trapping potential no longer holds.

In Fig. 3 the response of the photodiode is depicted as function of the position of the bead. Each curve corresponds to a different value of the capture angle of the condenser, θ_{cap} . The exact angle is stated in the legend. To minimize the effect of thermal fluctuations, each curve shows an average over 400 periods. An offset, increasing with θ_{cap} , has been subtracted to yield an output of 0 V at the equilibrium, defined as the mean axial position of the bead in the trap without external forces. The deviations from the linear regime are obvious in most cases when the bead is more than $\approx 0.5 \mu\text{m}$ away from the equilibrium. The legend also states the range in which the photodiode output changes linearly with the position of the bead. This range of linear detection has been defined as the minimal distance at which the difference between the bead position and the linear approximation is less than 30 nm.

We find that the range of linear detection is maximized at the lowest capture angle and is minimized for θ_{cap} between 35 and 44 deg. In the inset of Fig. 3 the sensitivity of the photodiode, defined as the slope of the output signal around 0 V, is plotted versus θ_{cap} . Here an optimal capture angle occurs at $\theta_{\text{cap}} = \theta_{\text{max}} \approx 26 \text{ deg}$. The minimal sensitivity appears when $\theta_{\text{cap}} = \theta_{\text{min}} = 40 \text{ deg}$, where the sensitivity is 0. It appears that the minimum in the linear detection range corresponds to a change in sign of sensitivity.

If needed, the position detection can be improved by including higher orders in the fit to the photodiode response. In this manner it appears that the measurement range is limited only by the presence of the inflection point in the photodiode output and can be extended up to 1 μm in the positive direction and even more in the negative direction at low θ_{cap} .

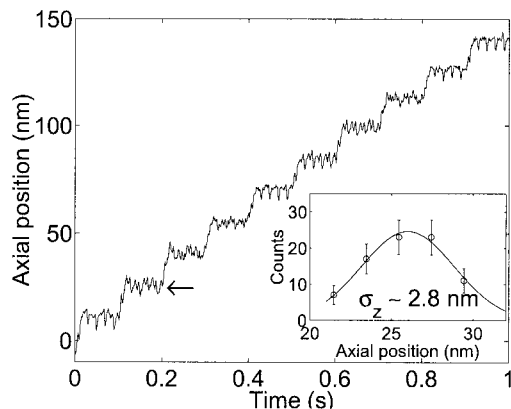


Fig. 4. Probing the spatial resolution of the position detection system by moving a fixed bead with the piezo stage in 14-nm steps in the axial direction. The inset shows a position histogram taken at a typical step (indicated by an arrow). The positions obtained indicate a resolution of 2.8 nm in the axial direction. The capture angle of the condenser was set to 35 deg.

However, at $\theta_{\text{cap}} = \theta_{\text{min}}$ no one-to-one mapping from the photodiode signal to position coordinates is possible.

To test the precision of the axial position detection, the response of the photodiode was measured as a fixed bead was moved in a controlled manner through the focus of the laser. For this measurement the best sensitivity was achieved with θ_{cap} equal to 35 deg. The beads were suspended in water containing 0.5 mM NaCl in order to attach the trapped bead to the coverslip: the bead was captured from the bulk of the solution and, while the distance to the coverslip was continuously decreased, the bead would at some point attach to the surface owing to the presence of the electrolyte. Care was taken not to perturb the equipment after the attachment of the bead to the coverslip to ensure that the bead was aligned laterally with respect to the beam axis.

Figure 4 shows the photodiode signal of the position of the immobilized bead when it was moved in 14 nm steps close to the focus of the laser. The individual steps, of duration 0.1 s, are easily distinguished. A typical step is indicated by an arrow in the figure. This step is investigated further to get the spatial resolution of the position detection system. A histogram over the positions in this step is shown in the inset of Fig. 4. A Gaussian fit to this histogram results in a standard deviation of 2.8 nm, which we take as the precision of the axial position detection. In some of the steps periodic noise at a frequency of 50 Hz is visible in the time series. This noise is probably caused by interference from nearby electronic installations.

5. Discussion

In Fig. 3 we demonstrate that the linear range and sensitivity of the axial position detection depends crucially on the aperture of the condenser. Similar results are found in the numerical work by Rohrbach

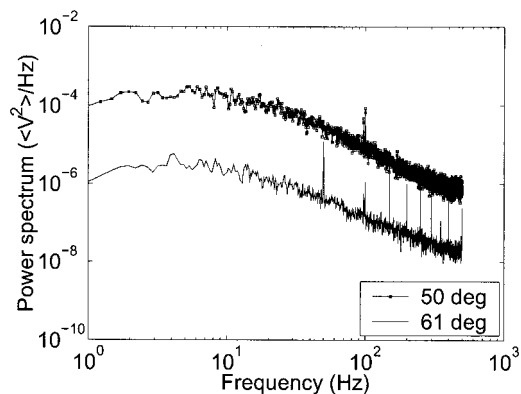


Fig. 5. Power spectra of the fluctuations of a trapped bead, recorded with the quadrant photodiode at various opening angles of the condenser. The increase in signal strength is ~ 2 orders of magnitude when the opening angle is decreased. Both signals have been high-pass filtered at 1 Hz. In the lower curve, the peaks are electronic noise, whereas in the upper curve only a 100 Hz peak is noticeable.

and Steltzer.¹¹ In their work, numerical simulations of the axial sensitivity of the photodiode with a trapped 150-nm polystyrene bead gave $\theta_{\text{min}} \approx 64$ deg. Furthermore, they found θ_{max} to be inversely proportional to $\sin(\theta_{\text{cap}})$, i.e., for axial position detection the optimal capture angle is as low as possible. We measure a definite θ_{max} , and when θ_{cap} is lowered below this angle the sensitivity in the axial position detection decreases. Furthermore, since the correlation values in Fig. 2(c) are approximately constant as function of angle below $\theta \approx 20$ deg, the sensitivity at low angles should be proportional to the photodiode area illuminated by the light cone of opening angle θ_{cap} , $\pi f \sin(\theta_{\text{cap}})^2$.

We may also, as a further documentation of our results, investigate the amplitude of the signal through a power spectral analysis. At a laser power similar to that of Fig. 2 we observe an 80-fold increase in power spectral density upon lowering the capture angle of the condenser from 61 to 35 deg; see Fig. 5. This demonstrates a significant increase in signal when our method is applied.

We found the exact values of θ_{max} and θ_{min} to be sensitive to parameters such as the depth of the laser trap in the sample, the laser intensity, and the size of the trapped bead. From the correlation measurement in Fig. 2(c), θ_{max} can be found as the angle where the correlation, $C(\theta)$, equals zero. When the detector area is integrated over angles smaller than this angle, only positively correlated regions contribute to the signal. From the plot in Fig. 2(c), θ_{max} is found to be ~ 35 deg. The variation in θ_{max} and θ_{min} is due to the fact that the equilibrium position of the trapped bead is shifted with respect to the geometrical focus of the trapping laser. The point at which the trapped bead is in equilibrium depends on the balance between the scattering of the laser beam, which tends to push the bead away from the focus point and the electrical field gradient of the focused

laser, which attracts the bead toward the focus point.¹² The relative strength of these opposing forces depends on details such as laser power and bead size. In the presence of spherical aberrations the equilibrium point may also depend on the depth in the sample.

The results reported in this paper apply when scattered light from the trapping laser beam itself is utilized for position detection. Areas of positive and negative correlation as in Fig. 2(b) and 2(c) are a result of the axial momentum transfer from the focused laser beam to the bead. This also indicates that position detection with a separate laser¹³ may have the same complex behavior only if it is as tightly focused as the trapping laser and shares the same focus plane in the sample. Thus it is most likely that position detection with a less tightly focused laser beam does not display the same critical dependence on θ_{cap} shown in Fig. 3.

6. Conclusion

The interference pattern in the back focal plane of the condenser lens behaves in a complex non-linear fashion with respect to the axial position of the trapped bead. As demonstrated, the axial position detection can be greatly improved both with respect to increased sensitivity and to the range of linear detection when the capture angle of the condenser is decreased to within 26–35 deg, the exact value depending on experimental conditions. When a large linear detection range is important, the capture angle should be as low as possible. Generally, when three-dimensional position detection is needed, one must find the aperture at which both axial and lateral positions are detected optimally. The experimental methods described above, the correlation measurement and the photodiode response experiment, are also easily applicable when optimizing lateral position detection, and, in fact, wherever position detection relies on interference.

We thank Christoph F. Schmidt and Poul Martin Hansen for useful discussions. This work was supported by the NKT Academy and the Danish Research Council.

References

1. M. J. Lang and S. M. Block, "Resource letter: Lbot-1: laser-based optical tweezers," *Am. J. Phys.* **71**, 201–215 (2003).
2. L. Oddershede, J. K. Dreyer, S. Grego, S. Brown, and K. Berg-Sørensen, "The motion of a single molecule, the λ -receptor, in the bacterial outer membrane," *Biophys. J.* **83**, 3152–3161 (2002).
3. M. D. Wang, Hong Yin, R. Landick, J. Gelles, and S. M. Block, "Stretching DNA with optical tweezers," *Biophys. J.* **72**, 1335–1346 (1997).
4. A. R. Clapp and R. B. Dickinson, "Direct measurement of static and dynamic forces between a colloidal particle and a flat surface using a single-beam gradient optical trap and evanescent wave light scattering," *Langmuir*, **17**, 2182–2191 (2001).
5. E.-L. Florin, A. Pralle, J. K. H. Hörber, and E. H. K. Stelzer, "Photonic force microscope based on optical tweezers and two-photon excitation for biological applications," *J. Struct. Biol.* **119**, 202–211 (1997).
6. F. Gittes and C. H. Schmidt, "Interference model for back-focal-plane displacement detection in optical tweezers," *Opt. Lett.* **23**, 7–9 (1998).
7. L. P. Ghislain, N. A. Switz, and W. W. Webb, "Measurement of small forces using an optical trap," *Rev. Sci. Instrum.* **65**, 2762–2768 (1994).
8. A. Pralle, M. Prummer, E.-L. Florin, E. H. K. Stelzer, and J. K. H. Hörber, "Three-dimensional high-resolution particle tracking for optical tweezers by forward scattered light," *Microsc. Res. Tech.* **44**, 378–386 (1999).
9. L. Oddershede, S. Grego, S. Nørrelykke, and K. Berg-Sørensen, "Optical tweezers: probing biological surfaces," *Probe Microsc.* **2**, 129–137 (2001).
10. K. Berg-Sørensen and H. Flyvbjerg, "Power spectrum analysis for optical tweezers," *Rev. Sci. Instrum.* (to be published).
11. A. Rohrbach and E. H. K. Stelzer, "Three-dimensional position detection of optically trapped dielectric particles," *J. Appl. Phys.* **91**, 5474–5488 (2002).
12. K. Svoboda and S. M. Bloch, "Biological applications of optical forces," *Annu. Rev. Biophys. Biomol. Struct.* **23**, 247–285 (1994).
13. K. Visscher and S. M. Block, "Versatile optical traps with feedback control," *Meth. Enzymol.* **298**, 460–489 (1998).